A First Look at the Thermal Neutron Scattering Law for H-UH_3

Michael L. Zerkle

Naval Nuclear Laboratory, PO Box 79, West Mifflin, PA 15122 USA
michael.zerkle@unnpp.gov

INTRODUCTION

Highly-enriched UH_3 has been used in several critical experiments [1,2]. Analyses of these experiments have historically ignored the effect of thermal neutron scattering in UH_3. In this paper the thermal neutron scattering law (TSL) for hydrogen bound in UH_3 (H-UH_3) is developed using the *ab initio* approach [3] as the first step in an effort to assess of the impact of the H-UH_3 TSL on the calculated k_{eff} for HEU-COMP-INTER-003 [2]. First-principles density functional theory and lattice dynamics calculations are used to calculate the dispersion relations and partial phonon density of states for UH_3. The GGA+U exchange correlation with spin-polarized magnetism is used to simulate the electronic structure of UH_3 with a Hubbard U parameter selected to reproduce experimental lattice constant measurements. The partial phonon density of states from these calculations is used to develop the TSL for H-UH_3 in the incoherent approximation.

CRYSTAL STRUCTURE AND LATTICE DYNAMICS

In the solid state, uranium hydride exists mainly in the form of a cubic trihydride (Pm3n symmetry group) with two allotropes: α-UH_3 and β-UH_3. The crystal structures for α- and β-UH_3 are shown in Figures 1 and 2, respectively, where the large (blue) and small (grey) balls denote U and H atoms. α-UH_3 is believed to be metastable and is only found at low (cryogenic) temperatures [4]. β-UH_3 is found at room temperature and above.

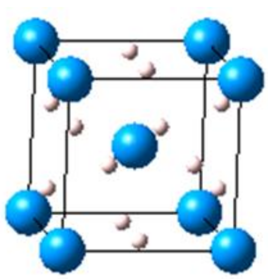

Fig. 1. The α-UH_3 unit cell.

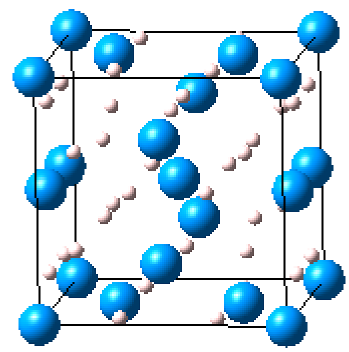

Fig. 2. The β-UH_3 unit cell.

α-UH_3 has a lattice constant of 4.16 Å [4] with two molecules (8 atoms) per unit cell. The two uranium atoms are equivalent and occupy positions (0,0,0) and (½, ½, ½), and there are six hydrogen atoms at ±(¼, 0, ½). Each uranium atom is surrounded by twelve hydrogen atoms at 2.32 Å.

β-UH_3 has a lattice constant of 6.643 ± 0.001 Å [5] with eight molecules (32 atoms) per unit cell. The uranium atoms are located as in β-tungsten with $2U_I$ at (0,0,0) and (½, ½, ½) and $6U_{II}$ at ±(¼, 0, ½). Each U_I atom is surrounded by twelve hydrogen atoms at the corners of an icosahedrons and each U_{II} atom is surrounded by twelve hydrogen atoms in sets of three, each set forming a face of a different icosahedron. All of the U-H distances are 2.32 Å [6].

First-principles quantum mechanics electronic structure simulations were performed using the *Vienna Ab-Initio Simulation Package* (VASP) density functional theory (DFT) code [7,8] to predict the crystal structure and Hellmann-Feynman forces of β-UH_3. The ground-state lattice structure was optimized using a total electronic energy threshold of 10^{-6} eV, planewave cutoff of 500 eV, k-point spacing of 0.2 $Å^{-1}$ (5×5×5 k-mesh), spin-polarized magnetism, and a pseudopotential based on the generalized gradient approximation (GGA) of Perdew, Burke and Ernzerhof (PBE) [9] for the exchange-energy correlation. A Hubbard U parameter correction was applied to the uranium 5f electrons to account for the effect of their strong-correlation on chemical binding. As shown in Fig. 3, a Hubbard parameter of U = 1.2 eV yields a lattice parameter of a = 6.6458 Å which is consistent with (0.04% higher than) the measured lattice parameter of a = 6.643 Å [5].

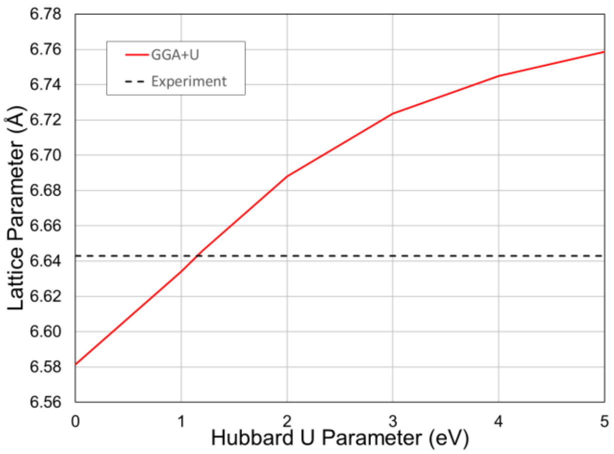

Fig. 3. Structure optimization of UH_3 using GGA+U. Hubbard parameter U = 1.2 eV yields lattice parameter consistent with experimental measurements.

Lattice dynamics calculations were performed to determine the dispersion relations and partial phonon density of states (DOS) for UH_3 using the PHONON code [10]. Interatomic Hellmann-Feynman forces on a 2×2×2 supercell (256 atoms) with ±0.02 Å asymmetric atom displacements were determined from VASP calculations using a k-point spacing of 0.02 Å^{-1} (3×3×3 k-mesh) for the PHONON supercell calculations.

Fig. 4 shows the calculated dispersion relations for UH_3 along the highest-symmetry points of the Brillouin zone derived from the PHONON calculations. The lower branches are acoustic modes which are mainly due to the heavy U atom vibrations. The higher branches are optical modes mainly due to the lighter H atom vibrations. Fig. 5 provides the calculated partial phonon DOS for H and U in UH_3. The phonon DOS has two well-separated regions due to the large mass ratio between U and H. The acoustic region (0.0-0.021 eV) is preferred for U atom vibrations and a broad optical region (0.078-0.160 eV, centered about 0.120 eV) is preferred for H atom vibrations. The calculated UH_3 optical region is consistent with published inelastic scattering measurements. In 1966, Rush *et al.* [11] found a broad optical mode centered about 970 cm^{-1} (0.120 eV) using low-resolution inelastic scattering measurements. More recently, high-resolution inelastic neutron scattering measurements of UH_3 by Glogolenko *et al.* [12] also found a broad optical mode centered about 0.120 eV (Fig. 6) and a shape consistent with the calculated phonon DOS.

Fig. 7 compares the phonon DOS for H-UH_3, H-PuH_2 [13], H-YH_2 [14], (calculated by Naval Nuclear Laboratory) and H-ZrH_2 [15] (calculated by General Atomics). All phonon DOS have been normalized on a consistent basis. The optical mode for H-UH_3 is considerably broader than the other metal hydrides. As will be shown in the next section, this difference in the shape of the phonon DOS has an impact on the shape of the multiphonon scattering peaks in the inelastic and total scattering cross sections.

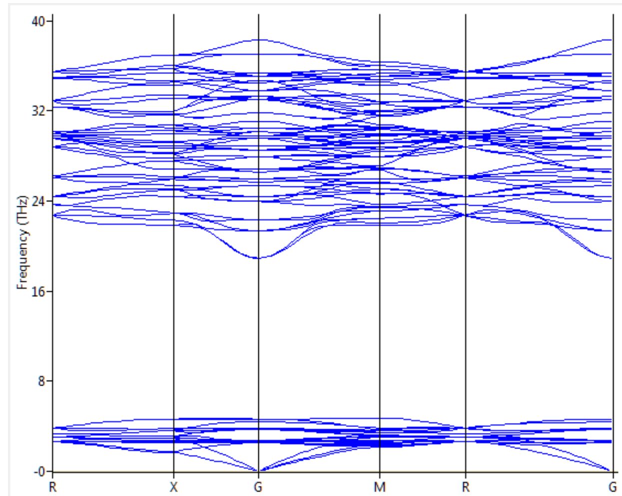

Fig. 4. Calculated dispersion relations for UH_3. (4.14 meV / THz)

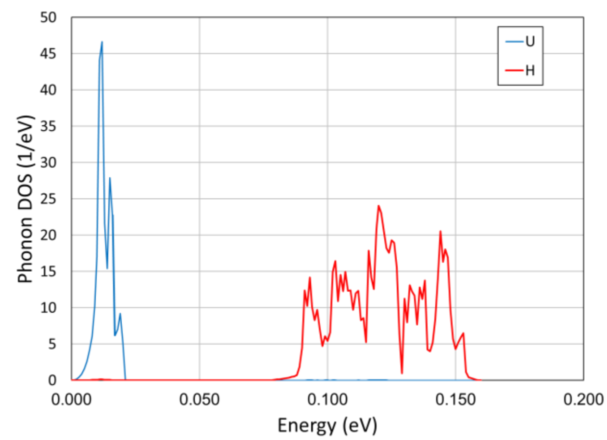

Fig. 5. Calculated partial phonon DOS for H and U in UH_3.

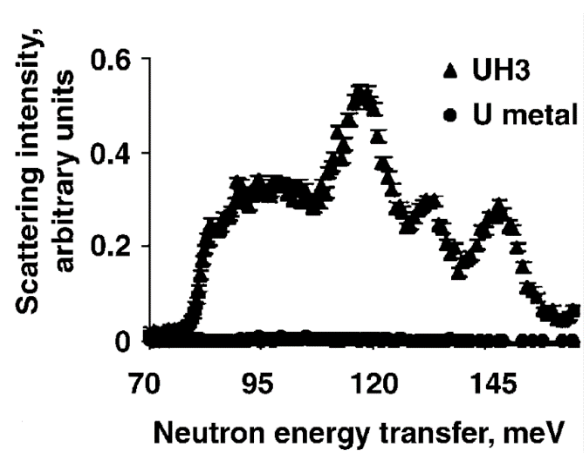

Fig. 6. UH_3 optical peak measured by Glogolenko *et al.* [12].

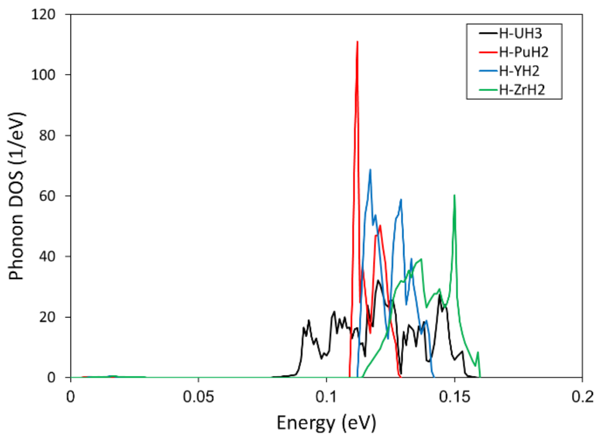

Fig. 7. Comparision of normalized calculated phonon DOS for H-UH_3, H-PuH_2, H-YH_2, and H-ZrH_2.

THERMAL NEUTRON SCATTERING LAWS

The TSL evaluation for H-UH_3 was developed from the calculated H partial phonon DOS for UH_3 using the LEAPR module of NJOY2012 [16]. ENDF/B-VII.1 atomic mass ratio and free atom scattering cross section for ^{1}H were used in the evaluation [17]. Inelastic scattering is treated in the incoherent approximation, and all elastic scattering is considered to be incoherent. The α (unitless momentum transfer) and β (unitless energy transfer) grids were optimized to represent thermal neutron scattering effects up to 5 eV. The total scattering, elastic scattering, and inelastic scattering cross sections for H-UH_3 at 293.6 K calculated by the NDEX [18] nuclear data processing system are shown in Fig. 8. The total scattering cross section for H-UH_3 converges to the free-atom scattering cross section for ^{1}H near 5 eV, as it theoretically should. The total and inelastic scattering cross sections for H-UH_3 contain oscillations due to multiphonon scattering similar to those present in the TSLs for other metal hydrides. Fig. 9 provides similar plots of the inelastic and elastic scattering cross sections for H-UH_3 from the THERMR module of NJOY2012. As has previously been noted for H-YH_2 [14] and H-PuH_2 [13], the automatic meshing algorithm in THERMR has difficulty resolving multiphonon scattering peaks beyond the second peak.

Fig. 10 compares the total scattering cross sections for H-UH_3, H-PuH_2, H-YH_2, and H-ZrH_2. The differences in the phonon DOS produce noticeable differences in the scattering cross sections. The multiphonon scattering peaks in H-UH_3 are not as pronounced as in the other metal hydrides.

CONCLUSIONS

The TSL for H-UH_3 has been evaluated using the *ab initio* approach. The calculated phonon DOS for UH_3 is consistent with published inelastic neutron scattering measurements. The broader optical mode results in shallower multiphonon peaks in the H-UH_3 inelastic and total scattering cross sections relative to the other metal hydrides that have been evaluated.

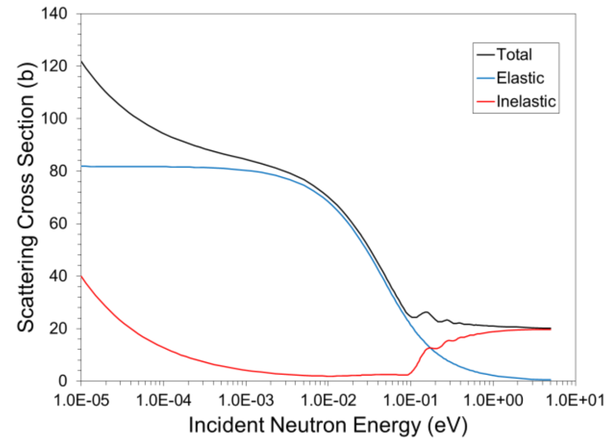

Fig. 8. Total, elastic, and inelastic scattering cross section for H-UH_3 at 293.6 K from NDEX.

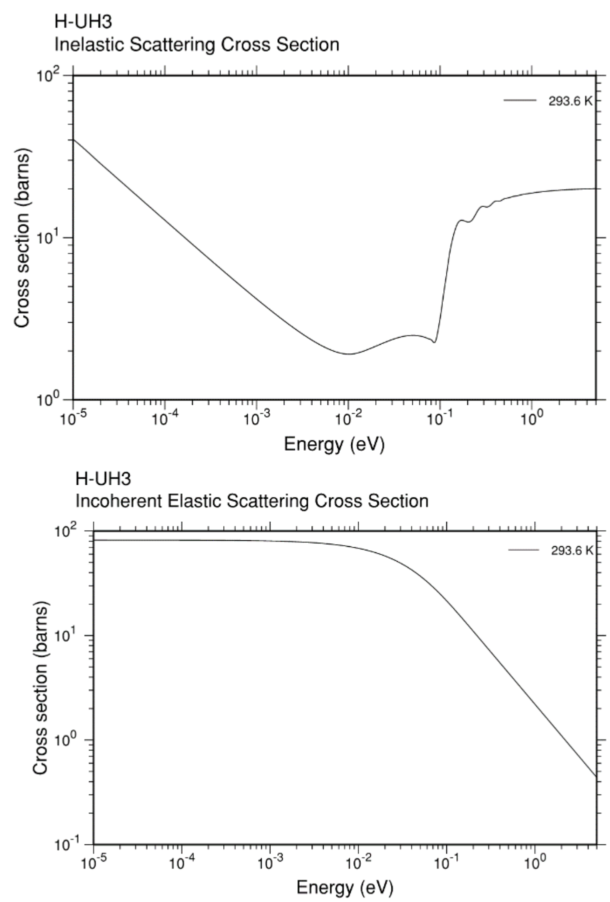

Fig. 9. Inelastic scattering (top) and incoherent elastic scattering (bottom) cross sections for H-UH_3 at 293.6 K from THERMR.

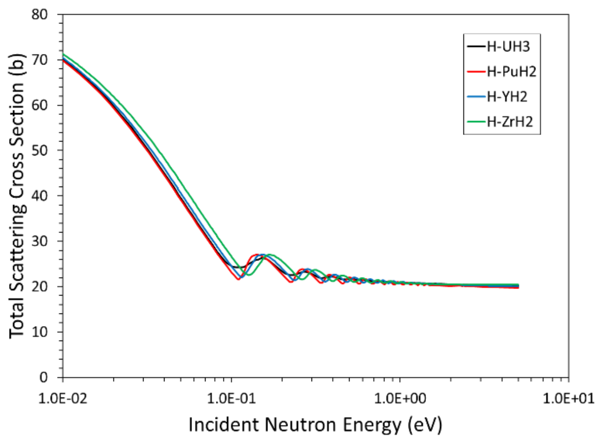

Fig. 10. Comparision of the total scattering cross sections for H-UH_3, H-PuH_2, H-YH_2, and H-ZrH_2 calculated by NDEX.

REFERENCES

1. G. A. LINENBERGER, J. D. ORNDOFF, and H. C. PAXTON, "Enriched-Uranium Hydride Critical Assemblies," *Nucl. Sci. Eng.*, **7**, 44-57 (1960).
2. R. BREWER and R. LABAUVE, "Reflected Uranium-Hydride Cylindrical Assemblies," HEU-COMP-INTER-003, *International Handbook of Evaluated Criticality Safety Experiments*, NEA/NSC/DOC(95)03, OECD/NEA, September 2016.
3. A. I. HAWARI et al., "Ab Initio Generation of Thermal Neutron Scattering Cross Sections," *Proc. PHYSOR 2004*, Chicago, Illinois, April 25-29, 2004, American Nuclear Society (2004).
4. R. N. R. MULFORD, F. H. ELLINGER and W. H. ZACHARIASEN, "A New Form of Uranium Hydride," *J. Am. Chem. Soc.*, **76**, 297-298 (1954).
5. W. BARTSCHER, A. BOEUF, R. CACIUFFO, J. M. FOURNIER, W. F. KUHS, J. REBIZANT and F. RUSTICHELLI, "Neutron Diffraction Study of β-UH_3 and β-UD_3, *Solid State Comm.*, **53**, 423-426 (1985).
6. R. E. RUNDLE, "The Structure of Uranium Hydride and Deuteride," *J. Am. Chem. Soc.*, **69**, 1719-1723 (1947).
7. G. KRESSE and J. FURTHERMÜLLER, "Efficient Iterative Schemes for Ab Initio Total-Energy Calculations Using a Plane-Wave Basis Set," *Phys. Rev. B*, **54**, 11169 (1996).
8. G. KRESSE and J. FURTHERMÜLLER, "Efficiency of Ab-Initio Total Energy Calculations for Metals and Semiconductors Using a Plane-Wave Basis Set," *Comp. Mat. Sci*., **6**, 15 (1996).
9. J. P. PERDEW, K. BURKE and M. ERNZERHOF, "Generalized Gradient Approximation Made Simple," *Phys. Rev. Let*., **77**, 3865-3868 (1996).
10. K. PARLINSKI *et al*., "First-Principles Determination of the Soft Mode in Cubic ZrO_2," *Phys. Rev. Let*., **78**, 4063-4066 (1997).
11. J. J. RUSH et al., Vibration Spectra of Yttrium and Uranium Hydrides by Inelastic Neutron Scattering of Cold Neutrons, *J. Chem. Phys.*, **45**, 3817 (1966).
12. I. Y. Glagolenko et al., "Quantitative Analysis of UH_3 in U metal and UO_2 Matrices by Neutron Vibrational Spectroscopy," *Appl Phys. A*, **74**, S1397-S1399 (2002).
13. M. L. ZERKLE and J. C. HOLMES, "The Thermal Neutron Scattering Law for Hydrogen Bound in Plutonium Dihydride and Predicted Critical Mass for Several Configurations," *Proc. 2017 NCSD Topical*, Carlsbad, New Mexico, September 10-15, 2017, American Nuclear Society (2017) (CD-ROM).
14. M. ZERKLE and J. HOLMES, "A Thermal Neutron Scattering Law for Yttrium Hydride," *EPJ Web of Conf.*, **146**, 13005 (2017).
15. E. L. SLAGGIE, "Central Force Lattice Dynamical Model for Zirconium Hydride," GA-8132, General Atomics (1967).
16. A. C. KAHLER, Ed., "The NJOY Nuclear Data Processing System, Version 2012," LA-UR-12-27079, Los Alamos National Laboratory (2012).
17. M. B. Chadwick et al., "ENDF/B-VII.1 Nuclear Data for Science and Technology: Cross Sections, Covariances, Fission Product Yields and Decay Data," *Nucl. Data Sheets*, **112**, 2887-2996 (2011).
18. D. P. GRIESHEIMER et al., "MC21 v.6.0 – A Continuous-Energy Monte Carlo Particle Transport Code with Integrated Reactor Feedback Capabilities," *Ann. Nucl. Energy*, **82**, 29-40 (2015).